Heavy Ion Physics at the LHC

R. Vogt

Nuclear Science Division, Lawrence Berkeley National Laboratory, Berkeley, CA 94720, USA
and
Physics Department, University of California, Davis, CA 95616, USA

- Exciting Initial State
- Hotter, Longer-Lived QGP
- Abundant Hard Probes
  - Quarkonium
  - Jets
  - Gauge Bosons
- Ultraperipheral Collisions

The LHC Probes Smallest x So Far Available

High energy pp and AA colliders probe successively smaller fractional momenta, x, of q, $\overline{q}$ and g for perturbative probes such as dijets, lepton pairs, gauge bosons or quarkonium produced at scale Q

$$x_1 = \frac{Q}{\sqrt{s_{NN}}} exp(y) \quad \text{“projectile”}$$
$$x_2 = \frac{Q}{\sqrt{s_{NN}}} exp(-y) \quad \text{“target”}$$

At the LHC, $|y| \leq 8.6 - 9.6$, depending on $\sqrt{s_{NN}}$

Very small x values can be probed, especially at forward rapidities since $\sqrt{s^{\rm LHC}_{\rm Pb+Pb}} \sim 30\sqrt{s^{\rm RHIC}_{\rm Au+Au}}$

The parton densities are unknown at such small x, even for the proton

Densities are dominated by gluons at low x, densities become extreme and growth must be tamed — multiplicities will not be as high as expected earlier ($dN^{\rm ch}/dy \sim 2000 - 3000$, not $dN^{\rm ch}/dy \sim 8000$)

Initial State a Soup of Gluons

High gluon densities lead to overlap and recombination of gluons, allowing some semi-classical description of low x regime such as a color glass condensate and/or nonlinear evolution of the parton densities

A semi-classical description allows calculation of the initial state

Such a regime will set in a higher x for nuclei than for protons due to larger R, $r_p \sim 0.8$ fm vs. $R_A \sim r_0 A^{1/3}$

Thus small x and the forward region interesting in their own right

However, it is imperative to measure proton and nuclear parton densities in pp and pA since initial state of AA collisions must be defined and understood

x and Q^2 Reach of Heavy Ion Machines

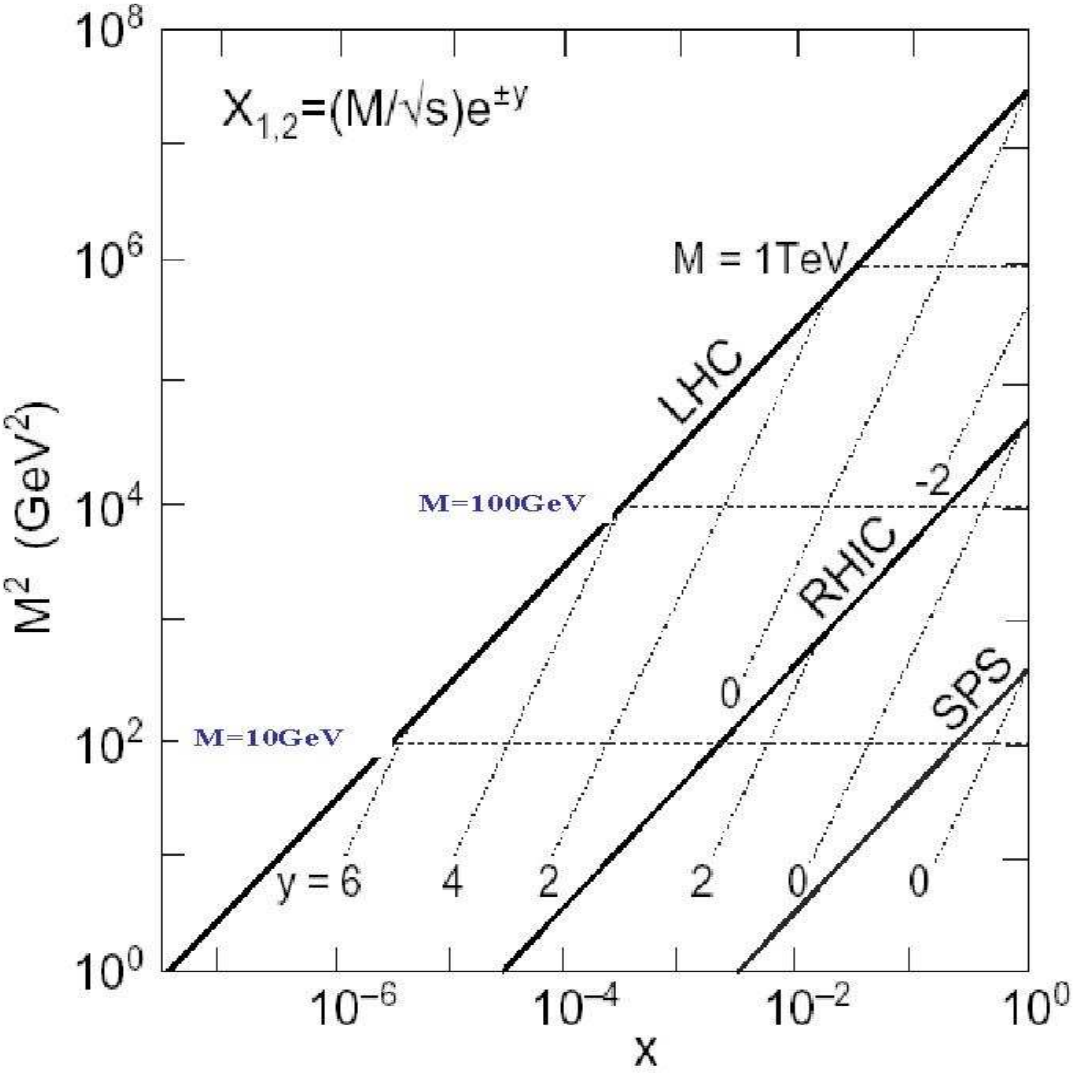

Figure 1: The $Q^2 = M^2 \geq 1$ GeV^2 reach as a function of x for the SPS, RHIC and the LHC. Lines of constant rapidity are indicated for each machine.

Possible x_2 Values for Range of Colliding Systems

Lowest x_2 values probed at forward rapidities

Need extended rapidity coverage to study full x_2 range

		$x_2(y, p_T)$					
	$\sqrt{s_{NN}}$	$y = 0$, p_T (GeV)		$y = 2$,p_T (GeV)		$y = 5$, p_T (GeV)	
System	(TeV)	2	10	2	10	2	10
Pb+Pb	5.5	$3.64 \cdot 10^{-4}$	$1.81 \cdot 10^{-3}$	$4.93 \cdot 10^{-5}$	$2.46 \cdot 10^{-4}$	$2.45 \cdot 10^{-6}$	$1.23 \cdot 10^{-5}$
Sn+Sn	5.84	$3.42 \cdot 10^{-4}$	$1.71 \cdot 10^{-3}$	$4.63 \cdot 10^{-5}$	$2.31 \cdot 10^{-4}$	$2.30 \cdot 10^{-6}$	$1.15 \cdot 10^{-5}$
Kr+Kr	6.14	$3.26 \cdot 10^{-4}$	$1.63 \cdot 10^{-3}$	$4.41 \cdot 10^{-5}$	$2.20 \cdot 10^{-4}$	$2.20 \cdot 10^{-6}$	$1.10 \cdot 10^{-5}$
Ar+Ar	6.3	$3.18 \cdot 10^{-4}$	$1.59 \cdot 10^{-3}$	$4.30 \cdot 10^{-5}$	$2.15 \cdot 10^{-4}$	$2.14 \cdot 10^{-6}$	$1.07 \cdot 10^{-5}$
O+O	7.0	$2.86 \cdot 10^{-4}$	$1.43 \cdot 10^{-3}$	$3.87 \cdot 10^{-5}$	$1.94 \cdot 10^{-4}$	$1.93 \cdot 10^{-6}$	$9.64 \cdot 10^{-6}$
pPb	8.8	$2.27 \cdot 10^{-4}$	$1.14 \cdot 10^{-3}$	$3.07 \cdot 10^{-5}$	$1.54 \cdot 10^{-4}$	$1.53 \cdot 10^{-6}$	$7.65 \cdot 10^{-6}$
pSn	9.0	$2.22 \cdot 10^{-4}$	$1.11 \cdot 10^{-3}$	$3.00 \cdot 10^{-5}$	$1.50 \cdot 10^{-4}$	$1.48 \cdot 10^{-6}$	$7.40 \cdot 10^{-6}$
pKr	9.27	$2.16 \cdot 10^{-4}$	$1.08 \cdot 10^{-3}$	$2.92 \cdot 10^{-5}$	$1.46 \cdot 10^{-4}$	$1.46 \cdot 10^{-6}$	$7.28 \cdot 10^{-6}$
pAr	9.39	$2.13 \cdot 10^{-4}$	$1.06 \cdot 10^{-3}$	$2.88 \cdot 10^{-5}$	$1.44 \cdot 10^{-4}$	$1.44 \cdot 10^{-6}$	$7.18 \cdot 10^{-6}$
pO	9.9	$2.02 \cdot 10^{-4}$	$1.01 \cdot 10^{-3}$	$2.73 \cdot 10^{-5}$	$1.37 \cdot 10^{-4}$	$1.36 \cdot 10^{-6}$	$6.80 \cdot 10^{-6}$
pp	14	$1.43 \cdot 10^{-4}$	$7.14 \cdot 10^{-4}$	$1.93 \cdot 10^{-5}$	$9.67 \cdot 10^{-5}$	$9.62 \cdot 10^{-7}$	$4.81 \cdot 10^{-6}$

Table 1: The values of x_2, the nuclear momentum fraction at forward rapidity, for several values of y, $y = 0$, 2 and 5, and p_T, $p_T = 2$ and 10 GeV. Results are given for all planned AA and pA systems, along with pp, in order of increasing $\sqrt{s_{NN}}$.

Proton Parton Densities

CTEQ6M: typical linearly-evolved DGLAP NLO parton densities

Sea quark and gluon densities, $xf(x)/x$, increase with decreasing x

Eventually gluons must start to recombine to tame growth, perhaps leading to a Color Glass Condensate in the initial state

N.B. many x values reachable at the LHC are lower than the x range of this plot by factors of $10-100$ or more where densities are higher still!

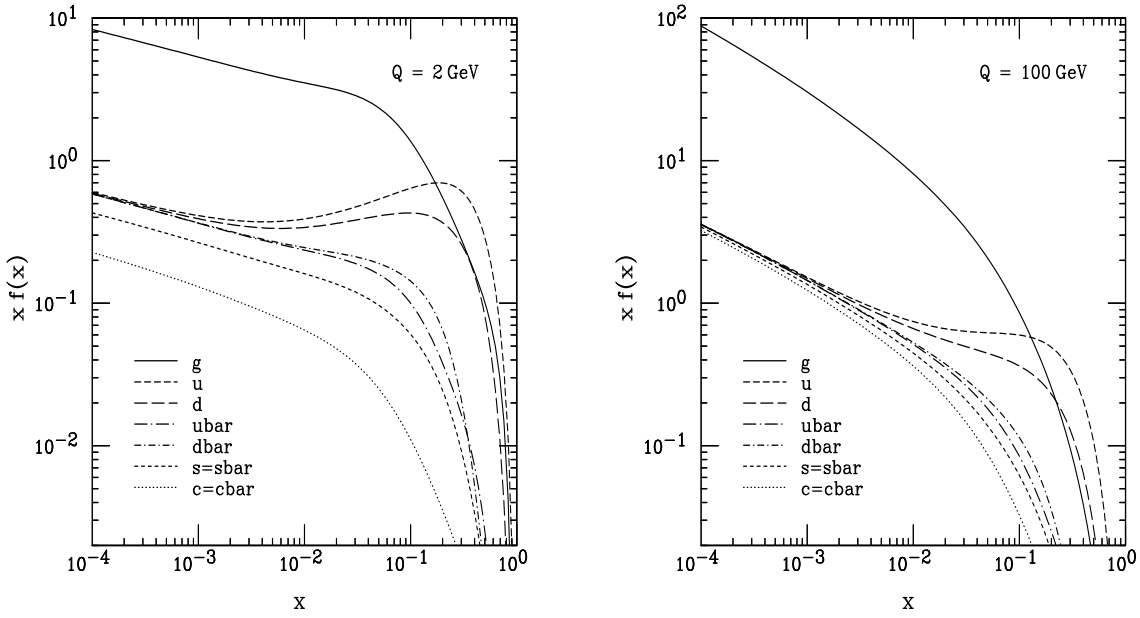

Figure 2: CTEQ6M parton distributions at $Q = 2$ and 100 GeV. [J. Pumplin *et al.*, JHEP 0207, 012 (2002), hep-ph/0201195.]

Parton Densities Modified in Nuclei

Interesting low x regime not probed for $Q^2 > 1$ GeV^2 for fixed-target energies

LHC can change that

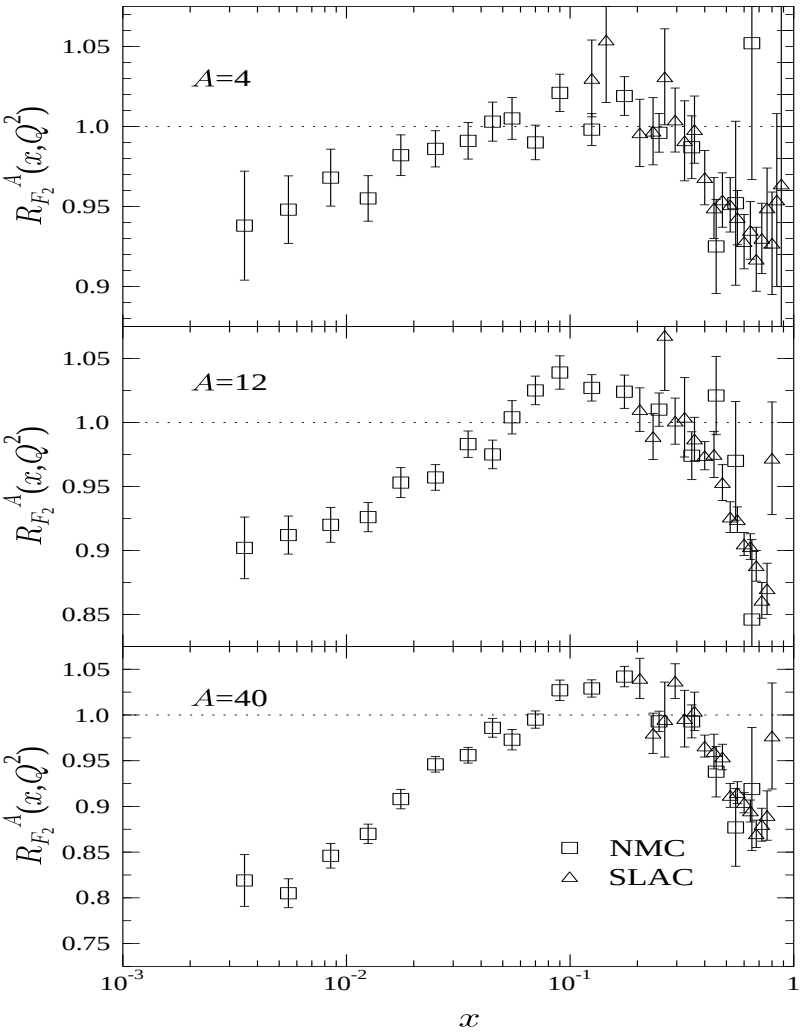

Figure 3: Ratios of charged parton densities in He, C, and Ca to D as a function of x. [From K.J. Eskola.]

BRAHMS Data Indicate the Importance of Initial State Effects

Shows that midrapidity suppression of R_{AA} is an initial-state effect

d+Au suppression increases at forward η where x becomes smaller

Intriguing centrality dependence, not very well understood

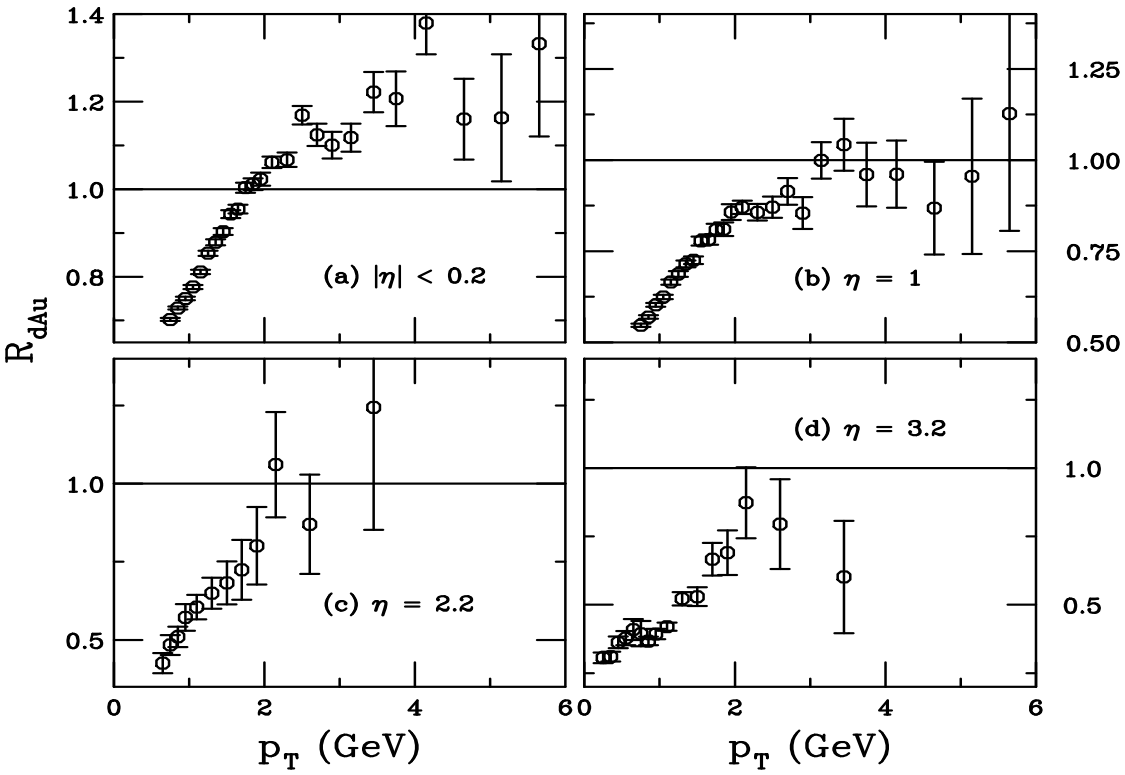

Figure 4: Ratio of d+Au charged particle distributions to those in pp at $\sqrt{s_{NN}} =$ 200 GeV in 4 bins of pseudorapidity. [From I. Arsene *et al.* [BRAHMS Collaboration], arXiv:nucl-ex/0403005.]

PHENIX J/ψ Data Show Modification of Nuclear PDFs

Not much effect at midrapidity

Suppression seen at forward η

Nuclear shadowing alone gives fair agreement with data

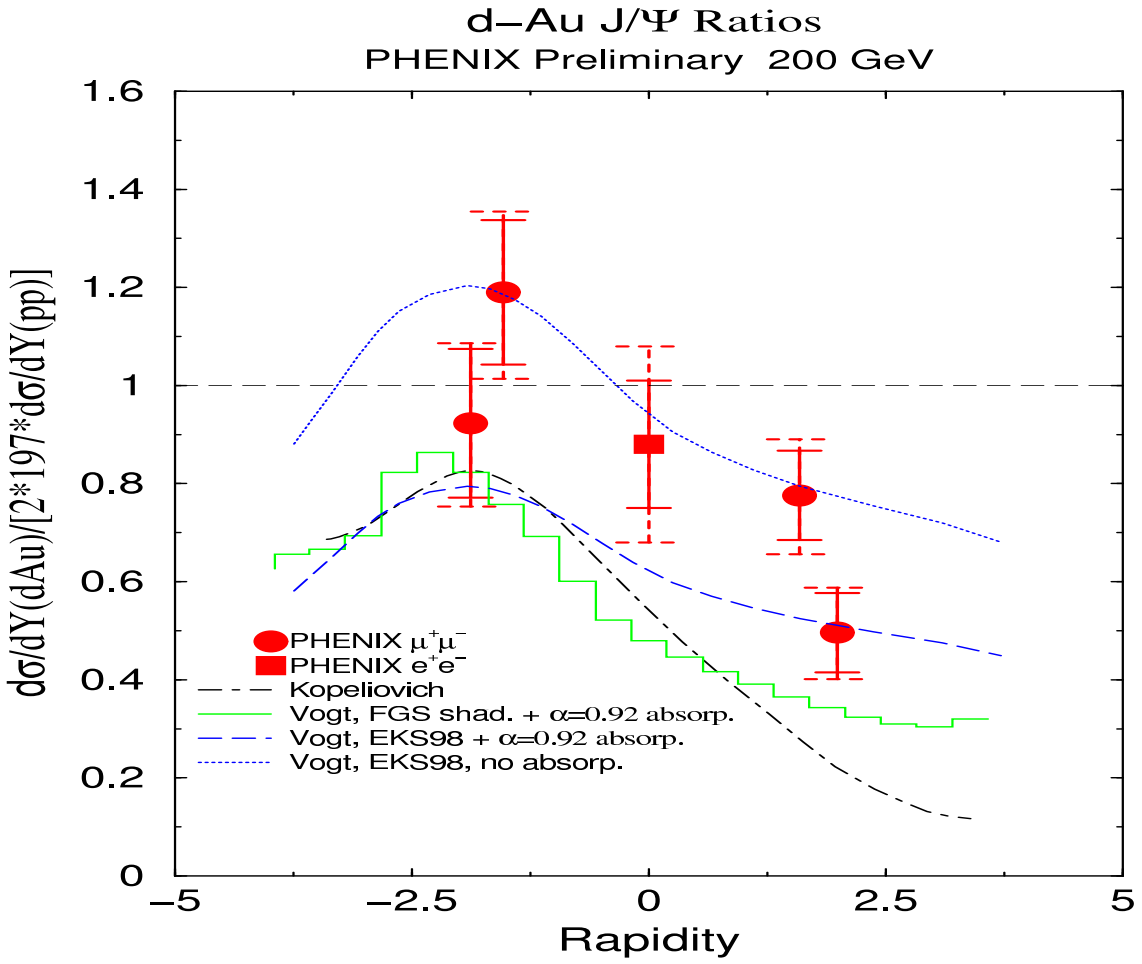

Figure 5: PHENIX d+Au/pp ratio for J/ψ production as a function of rapidity. The curves are theory calculations. The upper curve is EKS98 shadowing with no absorption. The lower shadowing curves have nuclear absorption added in by scaling the shadowing curves by A^{α} with $\alpha = 0.92$. [From PHENIX Collaboration, QM'04 proceedings.]

.

Midrapidity Region at LHC Baryon Free

Valence quarks and baryon number swept away from midrapidity to fragmentation regions

Manifestation of baryon number removal is in $\overline{p}/p$ ratio — $\overline{p}/p \to 1$ at high energies

Data seems to be consistent with this trend

- $\overline{p}/p \ll 1$ at SPS ($\sqrt{s_{NN}} \sim 17 - 20$ GeV
- $\overline{p}/p \sim 0.65$ at RHIC ($\sqrt{s_{NN}} = 130$ GeV)
- $\overline{p}/p \sim 0.77$ at RHIC ($\sqrt{s_{NN}} = 200$ GeV)
- $\overline{p}/p \to 1$ at LHC ($\sqrt{s_{NN}} = 5500$ GeV)

QGP is Hotter, Denser, and Longer Lived at the LHC

Formation time, τ_0, is a factor of 3 shorter than RHIC

Total lifetime of QGP, τ_{tot}, is a factor of 3 longer than RHIC

Initial temperature, T_0, factor of two larger than RHIC

Initial energy density, ε_0, factor of 13 to 20 higher than at RHIC

System	$\sqrt{s_{NN}}$ (GeV)	τ_0 (fm)	τ_{tot} (fm)	T_0 (MeV)	ε_0 (GeV/fm^3)
SPS (Pb+Pb)	17	0.8	1.4 – 2	210 – 240	1.5 – 2.5
RHIC (Au+Au)	200	0.6	6 – 7	380 – 400	14 – 20
LHC (Pb+Pb)	5500	0.2	18 – 23	710 – 850	190 – 400

Table 2: The initial QGP production time, lifetime, initial temperature and energy density for the maximum energy and mass systems at the SPS, RHIC and the LHC. [From I. Vitev, QM'04 proceedings.]

Implications of Hotter, Longer Lived QGP on Signals

Hotter plasma implies longer lifetime of plasma phase

More time spent in QGP means stronger effects on hard probes

More jet quenching

Hot enough for Υ suppression or stronger effect on Υ', Υ'' with p_T

Need high rates for high p_T, high mass production to quantify effects

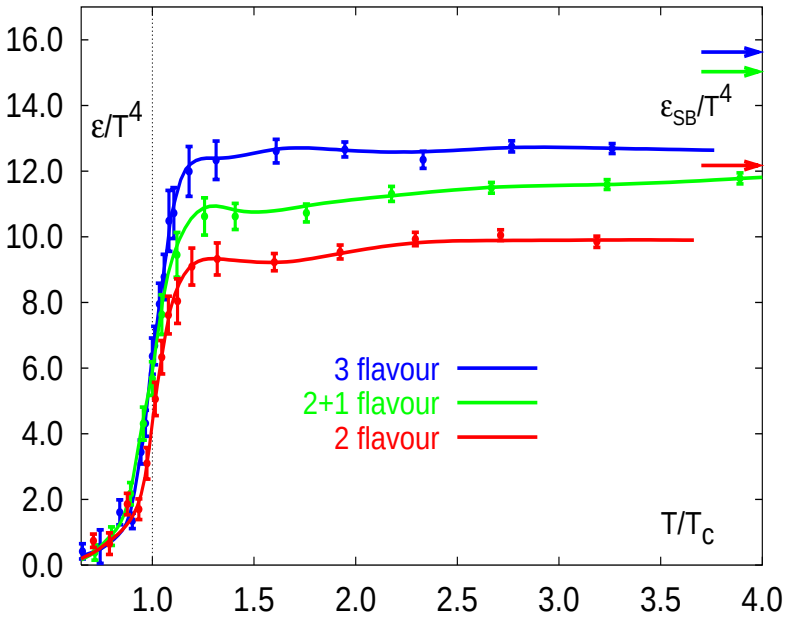

Figure 6: Energy density in QCD with staggered fermions for 2, $2+1$ and 3 flavors. Based on Vitev's numbers, $T_0^{\rm SPS} \sim 1.3T_c$, $T_0^{\rm RHIC} \sim 2.35T_c$ and $T_0^{\rm LHC} \sim (4-5)T_c$. [From F. Karsch, QM'01 proceedings.]

‘Hard’ Process

‘Hard’ processes have a large scale in the calculation that makes perturbative QCD applicable: high momentum transfer, μ^2, high mass, m, high transverse momentum, p_T

Understanding these processes relies on asymptotic freedom to calculate the interactions between two hadrons on the quark/gluon level but the confinement scale determines the probability of finding a particular parton in the proton

This implies factorization between the perturbative hard part and the universal, nonperturbative parton distribution functions

$$\sigma_{AB}(S) = \sum_{i,j=q,\overline{q},g} \int \frac{d\tau}{\tau} \int dx_1\, dx_2\, \delta(x_1 x_2 - \tau) \times f_i^A(x_1, \mu_F^2)\, f_j^B(x_2, \mu_F^2)\, \widehat{\sigma}_{ij}(s, \mu_F^2, \mu_R^2)$$

f_i^A are the parton distributions, either in a proton or a nucleus, determined from fits to data, x_1 and x_2 are the fractional momentum of the hadron carried by partons i and j, $\tau = s/S$

$\widehat{\sigma}_{ij}(s, \mu_F^2, \mu_R^2)$ is partonic cross section calculable in QCD in powers of α_s^{2+n}: leading order (LO), $n = 0$; next-to-leading order (NLO), $n = 1$ ...

High Yields of Hard Probes in Pb+Pb and pPb Collisions

	Pb+Pb $\sqrt{s_{NN}} = 5.5$ TeV $\mathcal{L} = 5 \times 10^{26}$ cm^{-2}s^{-1}	pPb $\sqrt{s_{NN}} = 8.8$ TeV $\mathcal{L} = 1.4 \times 10^{30}$ cm^{-2}s^{-1}
Process	Yield/10^6 s	Yield/10^6 s
$\lvert\eta\rvert \leq 2.4$		
jet($p_T > 50$ GeV)	2.2×10^7	1.5×10^{10}
jet($p_T > 250$ GeV)	2.2×10^3	5.2×10^6
Z^0	3.2×10^5	6.8×10^6
W^+	5.0×10^5	1.1×10^7
W^-	5.3×10^5	1.1×10^7
all phase space		
$c\bar{c}$	9.0×10^{10}	2.0×10^{12}
$b\bar{b}$	3.6×10^9	8.2×10^{10}
$J/\psi \to \mu^+\mu^-$	2.4×10^7	5.5×10^8
$\Upsilon \to \mu^+\mu^-$	1.5×10^5	3.5×10^6
$\Upsilon' \to \mu^+\mu^-$	3.7×10^4	8.4×10^5
$\Upsilon'' \to \mu^+\mu^-$	2.2×10^4	5.2×10^5

Table 3: The yield of hard probes in a 10^6 s LHC run. The numbers are based on reports from the CERN Yellow Report on Hard Probes of Heavy Ion Collisions at the LHC.

Quarkonium Production and Suppression

Matsui and Satz predicted J/ψ suppression

Normal absorption observed in pA, $\sigma_{pA} = \sigma_{pp} A^{\alpha}$ with $\alpha \sim 0.95$ (NA3, E537, E866, NA50, HERA-B)

Normal includes all cold nuclear matter effects: nucleon absorption, any scattering by comoving secondaries, nuclear shadowing effects, energy loss in cold matter, etc., all are wrapped up in α

NA50 sees absorption beyond the 'normal' at transverse energy $E_T > 30$ GeV

So far RHIC doesn't see any stronger absorption than NA50 as a function of the number of participants (but little data in Au+Au yet)

Whether this has anything to do with regeneration of J/ψ in the medium is unknown but is probably a small effect

If J/ψ's are regenerated, effect should be significant at LHC

$\Upsilon(1S)$ state is small, breakup by screening more difficult, good probe for LHC

NA50 Sees Anomalous J/ψ Suppression at the SPS

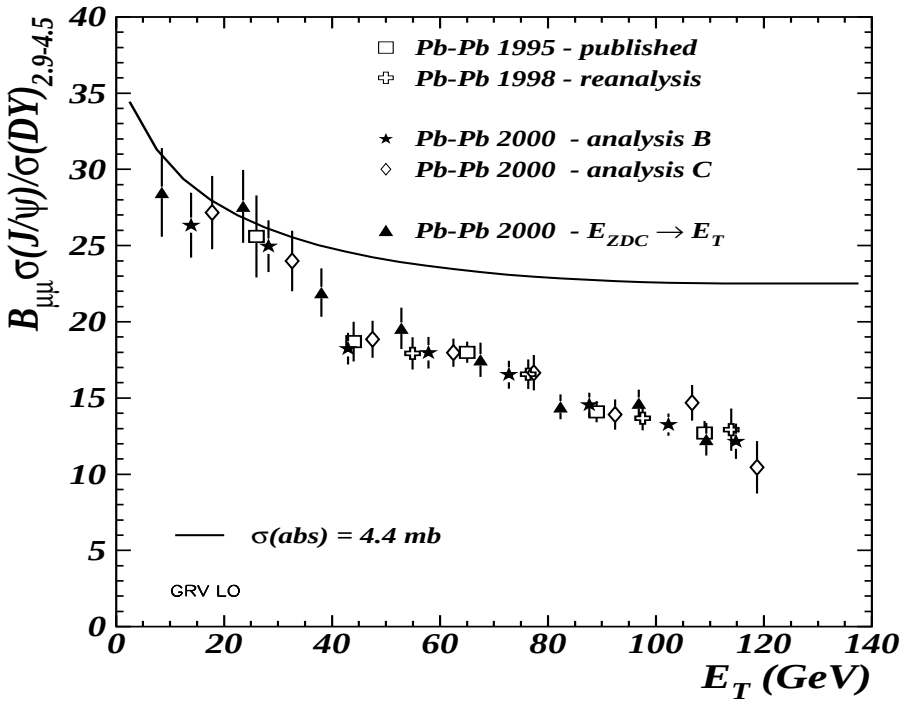

Figure 7: The J/ψ/Drell-Yan ratio from several years of NA50 results compared to the latest normal nuclear absorption curve with an absorption cross section of 4.4 mb. [From NA50, QM'02 proceedings.]

Simple Estimate of Maximum p_T For Suppression

Formation time of quarkonium states in lab

$$t_F = \tau_F \sqrt{1 + (p_T/M)^2}$$

$\tau_F^{J/\psi} = 0.92$ fm $\quad \tau_F^{\psi'} = 1.5$ fm $\quad \tau_F^{\chi_c} = 2.0$ fm
$\tau_F^{\Upsilon} = 0.76$ fm $\quad \tau_F^{\Upsilon'} = 1.9$ fm $\quad \tau_F^{\chi_b} = 2.6$ fm

Time center of system remains above T_c
assuming isentropic expansion, $s_D t_D(0) = s_0 t_0$

$$t_D(0) = t_0 \left(\frac{T_0}{T_c} \right)^3$$

Suppression occurs when $t_D(0)/t_F > 1$,
corresponding to a maximum p_T, $p_{T\,\mathrm{m}}$

$$p_{T\,\mathrm{m}} = M \sqrt{(t_D(0)/\tau_F)^2 - 1}$$

Survival Probability vs. p_T

Suppression pattern depends on initial conditions, system size, τ_F, and M

From entropy profile: $t_D(r) = t_D(0)(1-(r/R)^2)^{1/4}$
$R \leq R_{\rm Pb}$

Boundary of screening region: $r_S = R(1-(t/t_D(0))^{1/4})^{1/2}$

$Q\overline{Q}$ pair produced at $x^\mu = (0,\vec{r},0)$, $p^\mu = (\sqrt{M^2+p_T^2},\vec{p}_T,0)$

Quarkonium state formed at
$x^\mu = (\tau_F\sqrt{1+(p_T/M)^2},\vec{r}+\tau_F\vec{p}_T/M,0)$

State survives if $|\vec{r}+\tau_F\vec{p}_T/M| \geq r_S$

$$
\begin{aligned}
S(p_T) &= \frac{\int_0^R dr r\rho(r)\theta_(r,p_T)}{\pi\int_0^R dr r\rho(r)} \\
\rho(r) &= (1-(r/R)^2)^{1/2} \\
\theta(r,p_T) &= \begin{cases} \pi & z \leq -1 \quad \text{always survives} \\ \cos^{-1} z & |z|<1 \quad \text{sometimes survives} \\ 0 & z \geq 1 \quad \text{never survives} \end{cases} \\
z &= \frac{r_S^2 - r^2 - (\tau_F p_T/M)^2}{2r\tau_F p_T/M}
\end{aligned}
$$

Looking for QGP Characteristics via Quarkonium p_T Dependence

The ψ'/ψ and Υ'/Υ ratios are independent of p_T at the Tevatron (similar to color evaporation model predictions)

Effects of cold nuclear medium should be similar for ψ and ψ' and also for Υ, Υ' and Υ'': similar A dependence for each quarkonium type

Note that $\alpha_\psi \neq \alpha_{\psi'}$ (NA50, E866) but p_T-independent

Comover interactions should differ due to final state size but effect is small and not p_T dependent

No difference in shadowing effects expected for quarkonium states of the same family for color evaporation model (same x) but may be some small effect due to different singlet/octet production ratios for nonrelativistic QCD

Energy loss effects probably small for heavy quarks but loss occurs before hadronization

Thus only QGP production can significantly affect the p_T dependence of the ratios

Strongly dependent on initial conditions (Gunion and Vogt)

Some Sample Initial Conditions

Quarkonium breakup parameters taken from Karsch, Mehr and Satz

Parton gas estimates of initial conditions by Xu *et al.*

Minijet plasma based on minijet calculations by Eskola and Kajantie, generally higher T_0 but shorter lifetime from shorter t_0

	t_D (fm)	$p_{T\mathrm{m}}$ (GeV)	t_D (fm)	$p_{T\mathrm{m}}$ (GeV)
	$\mu \propto gT$, $n_f = 3$, $T_c = 170$ MeV		$\mu = 4T$, $T_c = 260$ MeV	
parton gas, $T_0 = 820$ MeV, $t_0 = 0.5$ fm				
ψ	4.12	13.96	15.69	54.0
ψ'	40.8	100.6	15.69	38.5
χ_c	48.9	85.47	15.69	27.2
Υ	-	0	4.6	56.53
Υ'	4.79	23.16	15.69	81.98
χ_b	8.90	32.42	15.69	58.9
minijet plasma, no shadowing				
	$T_0 = 820$ MeV, $t_0 = 0.1$ fm		$T_0 = 1.05$ GeV, $t_0 = 0.1$ fm	
ψ	-	0	6.59	22.7
ψ'	8.17	19.8	6.59	15.8
χ_c	9.78	16.75	6.59	11.0
Υ	-	0	1.94	22.2
Υ'	-	0	6.59	33.2
χ_b	-	0	6.59	23.05
minijet plasma, HPC shadowing				
	$T_0 = 699$ MeV, $t_0 = 0.1$ fm		$T_0 = 897$ MeV, $t_0 = 0.1$ fm	
ψ	-	0	4.11	13.8
ψ'	5.06	11.9	4.11	9.4
χ_c	6.06	10.0	4.11	6.3
Υ	-	0	1.21	11.7
Υ'	-	0	4.11	19.2
χ_b	-	0	4.11	12.1

Table 4: Values of t_D and $p_{T\mathrm{m}}$ for $\mu(T) \propto gT$ and $\mu(T) = 4T$ for several sets of initial conditions. [After J.F. Gunion and R.V., Nucl. Phys. **B492** (1997) 301.]

Charmonium Production Cross Sections

Difference between pp and pA, AA results at same energy due to EKS98 shadowing only, no absorption

Calculated in color evaporation model

		$\sigma^{\rm dir}$/nucleon pair (μb)				$B\sigma^{\rm inc}A^2$ (μb)	
System	$\sqrt{s}$ (TeV)	J/ψ	χ_{c1}	χ_{c2}	ψ'	J/ψ	ψ'
pp	14	32.9	31.8	52.5	7.43	3.18	0.057
pp	8.8	25.0	24.2	39.9	5.65	2.42	0.044
pPb	8.8	19.5	18.9	31.1	4.40	392.3	7.05
pp	7	21.8	21.1	34.9	4.93	2.11	0.038
O+O	7	17.6	17.0	28.1	3.98	436.2	7.84
pp	6.3	20.5	19.9	32.8	4.63	1.99	0.036
Ar+Ar	6.3	15.0	14.5	23.9	3.38	2321	41.7
pp	6.14	20.2	19.6	32.3	4.56	1.96	0.035
Kr+Kr	6.14	13.7	13.2	21.8	3.08	9327	167.6
pp	5.84	19.6	19.0	31.3	4.42	1.90	0.034
Sn+Sn	5.84	12.8	12.4	20.4	2.89	17545	315.2
pp	5.5	18.9	18.3	30.2	4.26	1.83	0.033
Pb+Pb	5.5	11.7	11.3	18.7	2.64	48930	879

Table 5: The direct cross section per nucleon pair and the dilepton cross section per nucleon multiplied by A^2 for the minimum bias lepton pair cross section. The results are given for $m_c = 1.2$ GeV, $\mu = 2m_T$ and the MRST HO parton densities. We compare pp to pA and AA interactions. [From the heavy flavor part of Hard Probes Yellow Report.]

Bottomonium Production Cross Sections

Difference between pp and pA, AA results at same energy due to EKS98 shadowing only, no absorption

Calculated in color evaporation model

		$\sigma^{\rm dir}$/nucleon pair (μb)					$B\sigma^{\rm inc}A^2$ (μb)		
System	$\sqrt{s}$ (TeV)	Υ	Υ'	Υ''	$\chi_b(1P)$	$\chi_b(2P)$	Υ	Υ'	Υ''
pp	14	0.43	0.27	0.16	0.89	0.69	0.020	0.0050	0.0030
pp	8.8	0.29	0.18	0.11	0.60	0.47	0.014	0.0040	0.0020
pPb	8.8	0.25	0.16	0.097	0.52	0.41	2.51	0.65	0.37
pp	7	0.23	0.15	0.090	0.48	0.38	0.011	0.0029	0.0016
O+O	7	0.21	0.13	0.081	0.44	0.34	2.57	0.66	0.38
pp	6.3	0.21	0.14	0.082	0.44	0.34	0.010	0.0026	0.0015
Ar+Ar	6.3	0.18	0.12	0.070	0.38	0.29	13.8	3.59	2.02
pp	6.14	0.21	0.13	0.080	0.43	0.33	0.0099	0.0026	0.0014
Kr+Kr	6.14	0.17	0.11	0.066	0.35	0.28	57.4	14.8	8.38
pp	5.84	0.20	0.12	0.076	0.41	0.32	0.0094	0.0024	0.0014
Sn+Sn	5.84	0.16	0.10	0.062	0.33	0.26	108.1	28.0	15.8
pp	5.5	0.19	0.12	0.070	0.39	0.30	0.0090	0.0020	0.0013
Pb+Pb	5.5	0.15	0.094	0.057	0.31	0.24	304	78.8	44.4

Table 6: The direct cross section per nucleon pair and the dilepton cross section per nucleon multiplied by A^2 for the minimum bias lepton pair cross section. The results are given for $m_b = 4.75$ GeV, $\mu = m_T$ and the MRST HO parton densities. We compare pp to pA and AA interactions.[From the heavy flavor part of Hard Probes Yellow Report.]

Prompt ψ'/ψ Ratios

Assume that direct J/ψ can be separated from ψ' and ψ decays, at least in pp and pA, as at Tevatron

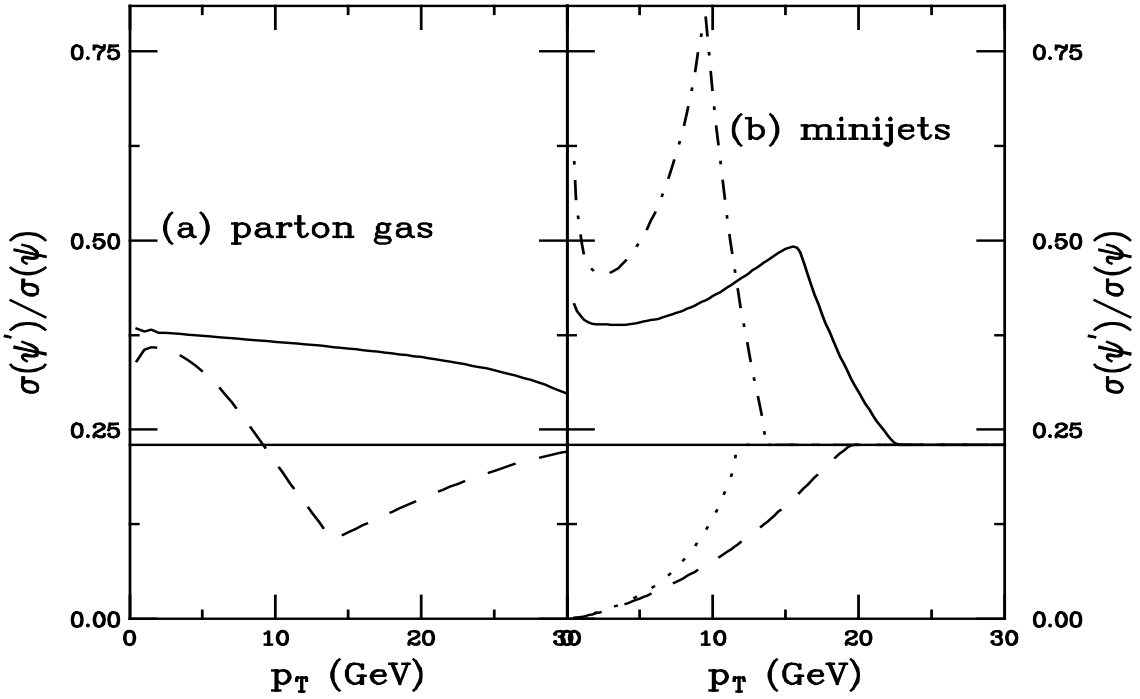

Figure 8: The direct or prompt ψ'/ψ ratio as a function of p_T is shown for several choices of initial conditions and $R = R_{\mathrm{Pb}}$. In (a), parton gas results are shown for $\mu \propto gT$ (dashed) and $\mu = 4T$ (solid). In (b) minijet results are given for both cases without shadowing, $\mu \propto gT$ (dashed) and $\mu = 4T$ (solid), and with shadowing, $\mu \propto gT$ (dotted) and $\mu = 4T$ (dot-dashed). The horizontal curve represents the pp ratio. [After J.F. Gunion and R.V., Nucl. Phys. **B492** (1997) 301.]

Indirect Υ'/Υ Ratios

Don't expect to tease out $\chi_b(1P)$ and $\chi_b(2P)$ contributions in heavy ion environment

$$\frac{\Upsilon'}{\Upsilon}\Big|_{\text{indirect}} \equiv \frac{\Upsilon' + \chi_b(2P)(\to \Upsilon') + \Upsilon''(\to \Upsilon')}{\Upsilon + \chi_b(1P,2P)(\to \Upsilon) + \Upsilon'(\to \Upsilon) + \Upsilon''(\to \Upsilon)}$$
$$= 0.53 \quad \text{(Tevatron data)}$$

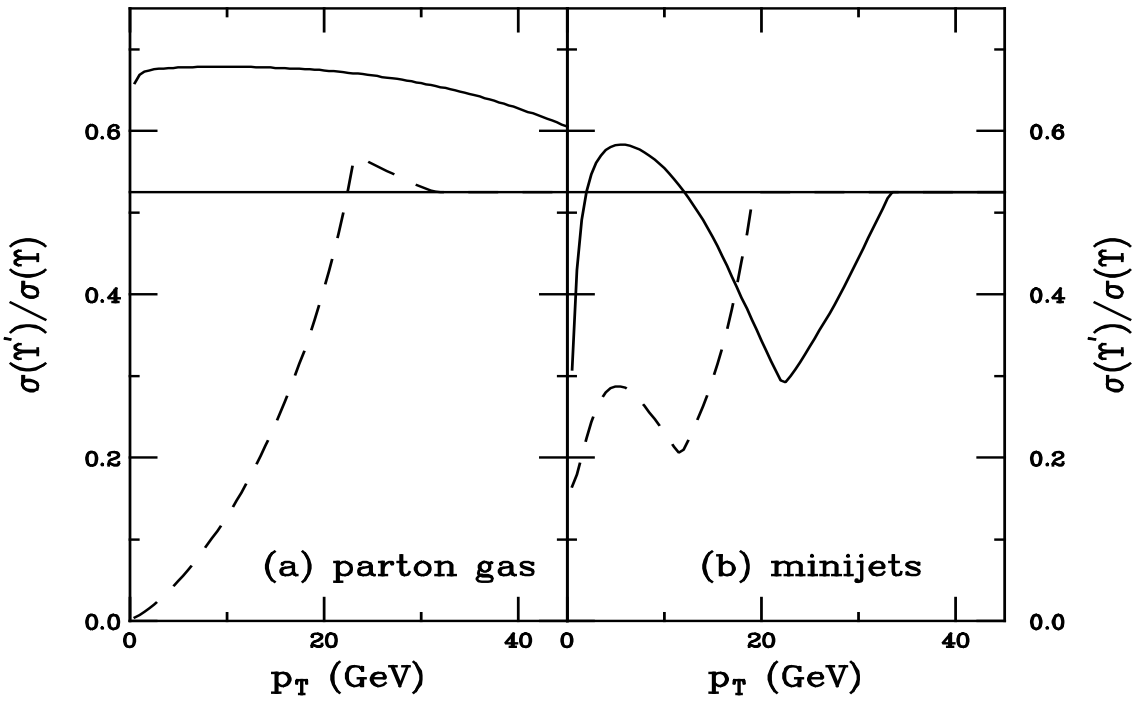

Figure 9: The Υ'/Υ ratio is shown for several initial conditions and $R = R_{\text{Pb}}$. In (a), parton gas results are shown for $\mu \propto gT$ (dashed) and $\mu = 4T$ (solid). In (b) minijet results are given for $\mu = 4T$ without (solid) and with (dashed) nuclear shadowing. The horizontal line represents the $p\overline{p}$ ratio. [After J.F. Gunion and R.V., Nucl. Phys. **B492** (1997) 301.]

Jet Probes

High p_T jets materialize after collision, $\tau \sim 1/p_T$

Embedded in and propagate through dense matter

Dijets normally produced back to back but if one jet escapes from surface and other must traverse medium, it gets modified relative to its partner

Change in azimuthal difference between two jets seen already in lower energy *pA* fixed-target experiment E609

Strong effect seen at RHIC

Nuclear Effects on Dijet Production from Fixed Target

Fermilab E609 pA at 400 GeV
$A =$ He, Be, C, Al, Cu, Sn, Pb

Required $p_T > 4$ GeV for each jet to reduce background

Measured $\Delta\phi$, azimuthal angle between jets, in pp and pA

Width of $\Delta\phi$ distributions used to obtain k_T, vector imbalance in p_T between jets

Determined standard deviation, σ, from Gaussian fit to $\Delta\phi$ distribution

$k_{T1} \approx p_T \sin\sigma$ is component of k_T in ϕ direction
Significant acoplanarity in pPb interactions

pp**:** $\sigma = 13^\circ$, $k_{T1} = 0.9 \pm 0.2$ GeV

p**Pb:** $\sigma = 24^\circ$, $k_{T1} = 2.0 \pm 0.2$ GeV

E609 Results

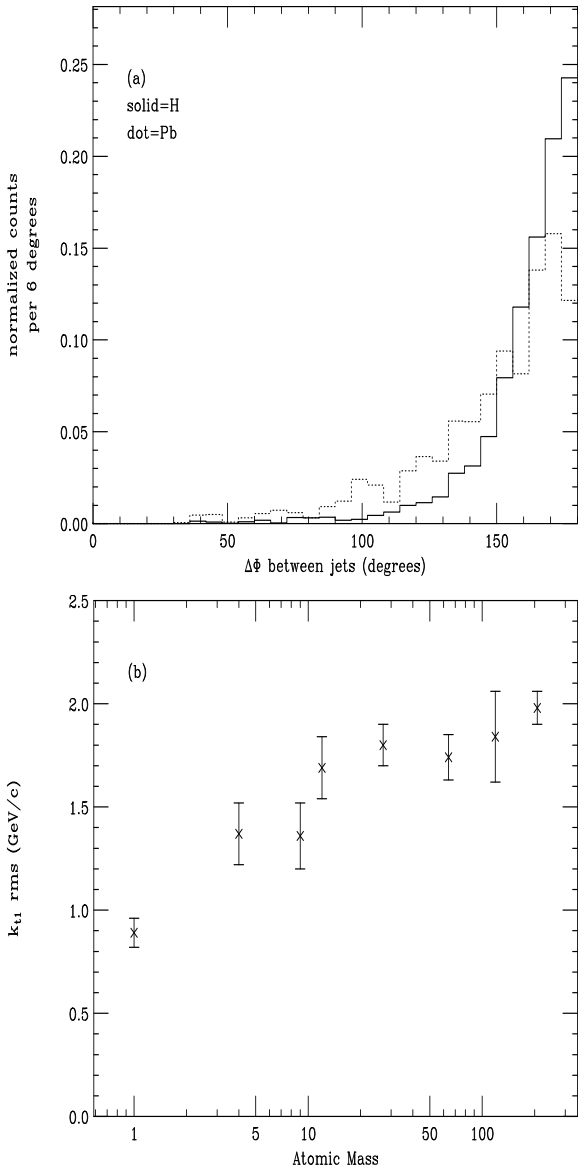

Figure 10: (a) The distribution in $\Delta\phi$. (b) The average value of k_{T1} as a function of A. The errors are statistical only. [From E609.]

STAR Dijet Results

In peripheral collisions (left-hand side), data agrees with pp + fbw

Central collisions, right-hand side, opposite side particle has disappeared, data goes with the fbw

But initial or final state effect?

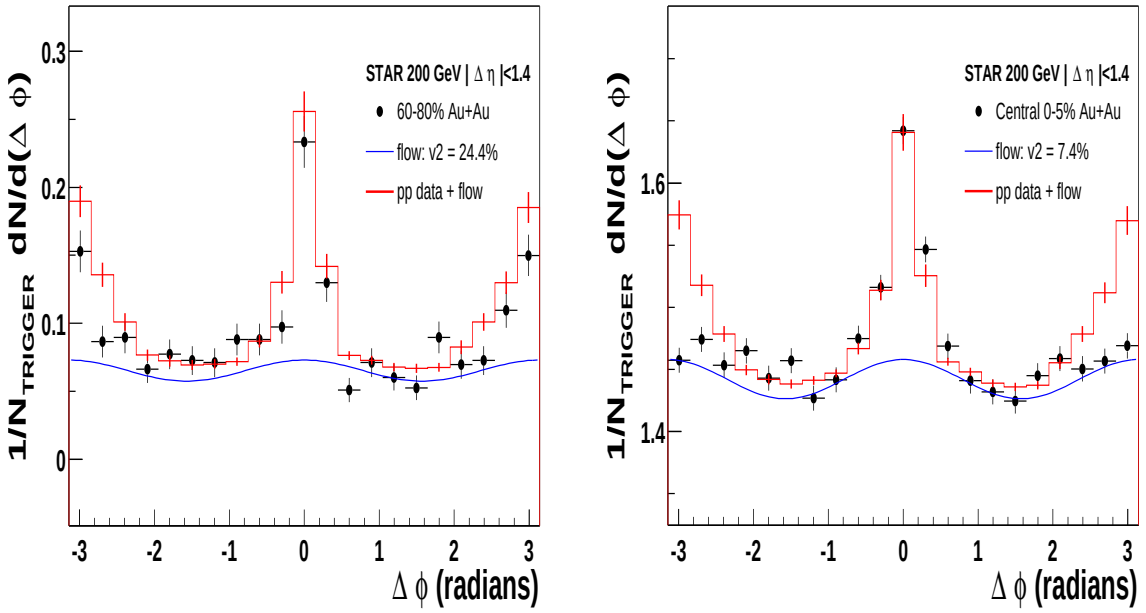

Figure 11: Azimuthal distributions of back-to-back high p_T particles in STAR. Compares the Au+Au results to pp data with a flow component added. The points are the data, the red histogram is pp + flow while the blue curve is the flow component alone. Note the difference in scales on the y-axes. Left-hand side: Peripheral (60 – 80%). Right-hand side: Central (0 – 5%). [From STAR Collab., Phys. Rev. Lett. **90** (2003) 082302.]

Jet Suppression a Final-State Effect

d+Au is control experiment, determines whether the disappearance of the opposite side hadron is an initial or final state effect

d+Au like *pp* so that Au+Au effect is in the final state, evidence for energy loss in the medium

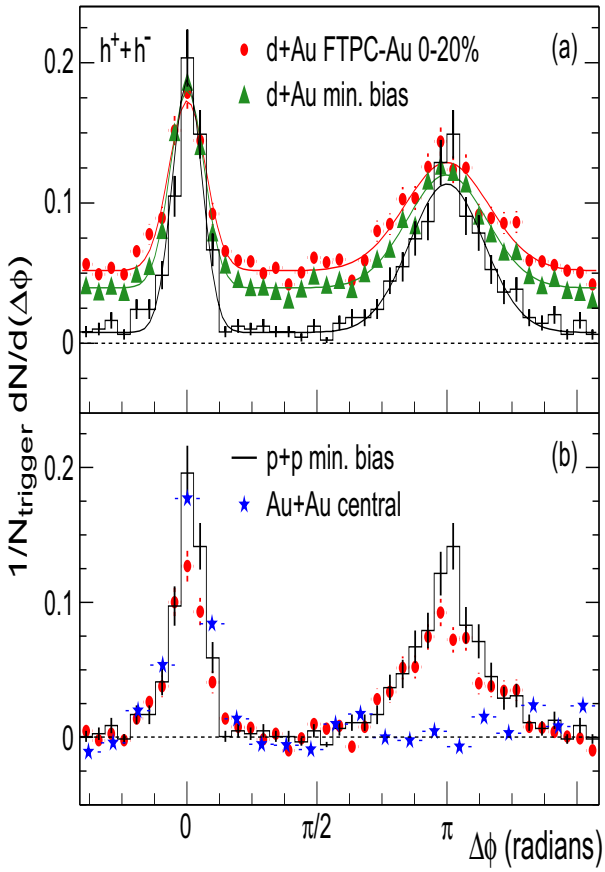

Figure 12: Comparison of azimuthal distributions in *pp* (solid histogram), d+Au (green triangles, min bias, and red circles, central) and Au+Au (blue stars) collisions at $\sqrt{s_{NN}} = 200$ GeV by STAR. [From STAR Collab., Phys. Rev. Lett. **91** (2003) 072304.]

γ+Jet More Direct Measure of Energy Loss

Dijet signals can be difficult because both jets may be modified by the passage through matter

Tag jets of known energy opposite a photon or Z^0 since these electroweak probes are unaffected by the medium, Z^0 would have less background but lower rate

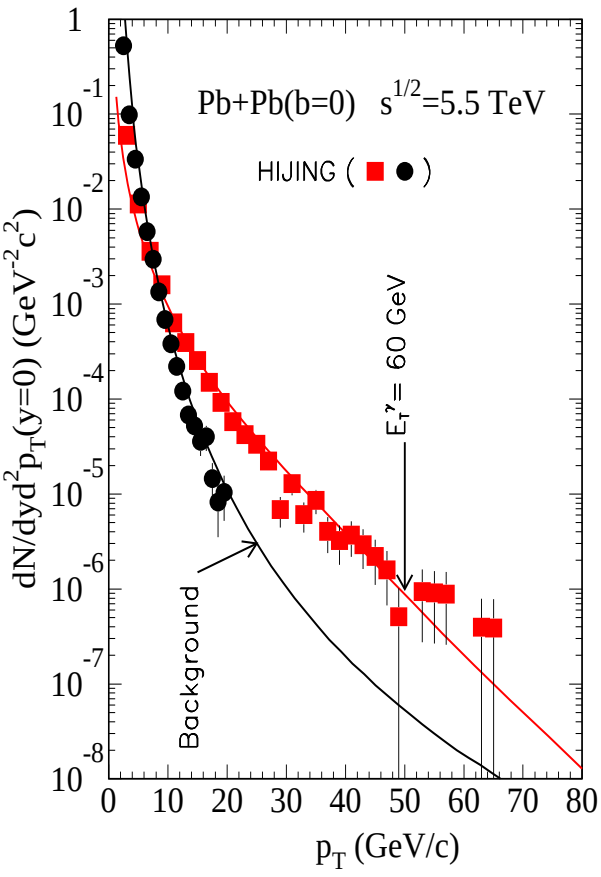

Figure 13: The p_T distribution of jets opposite photons with $E_T^\gamma = 60$ GeV compared to the underlying background in central Pb+Pb collisions at LHC. The direct photon and jet are restricted to the rapidity window $|y| \leq 0.5$. The jet is in the opposite direction to the photon. The solid curves and HIJING simulations assume no energy loss. Energy loss would decrease the jet rate by a factor of 2 at high p_T to 5 at low p_T. [From Wang and Huang.]

Other Jet Signals

Energy loss measures opacity of medium, providing access to produced parton density

Modification of fragmentation functions in the medium, compare high p_T components of jets in pp, p(d)A and AA

While energy loss effects on the total jet shape should be small, it should have a significant effect on the hadron multiplicty in the jet itself

Heavy quarks may experience less energy loss due to their mass, can be measured through flavor tagging of jets

Gauge Boson Production Useful for Measuring Nuclear PDFs at High Q^2

- No final state interactions
- Rate high, low background
- Dominated by $q\bar{q} \rightarrow Z^0$, $q\bar{q}' \rightarrow W^{\pm}$
- Strongly affected by nuclear isospin
- $x_1, x_2 \geq 0.02$, nuclear modifications small at midrapidity
- No change in m_{Z^0}, Γ_{Z^0} due to finite temperature (Kapusta and Wong)

Z^0 Shadowing in Pb+Pb at 5.5 TeV

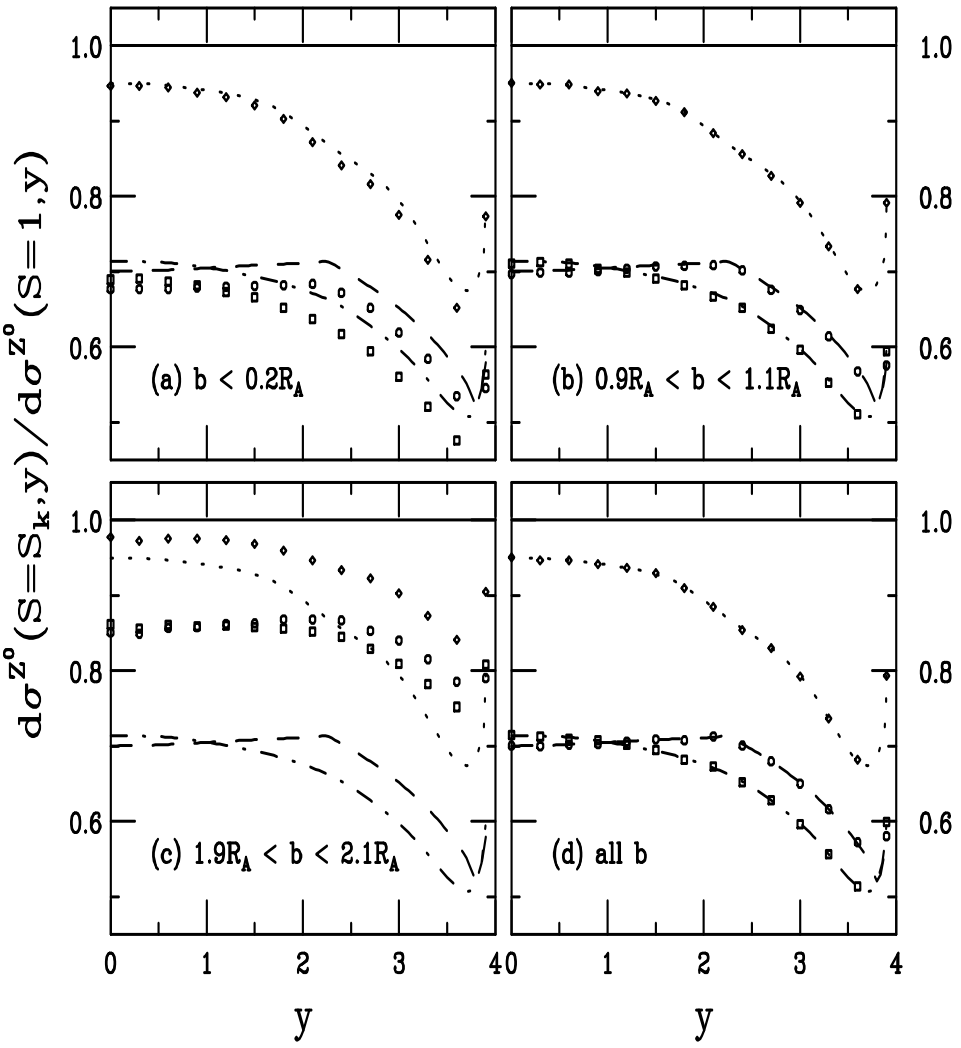

Figure 14: The Z^0 rapidity distributions, relative to $S = 1$ for Pb+Pb collisions, calculated with the MRST HO distributions. Central, $b < 0.2R_A$, semi-central, $0.9R_A < b < 1.1R_A$, peripheral, $1.9R_A < b < 2.1R_A$ impact parameters are shown along with the integral over all b. The homogeneous shadowing results are given in the dashed, HPC, dot-dashed, Eskola, and dotted, EKS98, lines. The inhomogeneous shadowing ratios for HPC, circles, Eskola, squares, and EKS98, diamonds, are also shown. [R.V., Phys. Rev. **C64** (2001) 044901.]

Gauge Boson Shadowing in *p*Pb and Pb*p* at 5.5 TeV

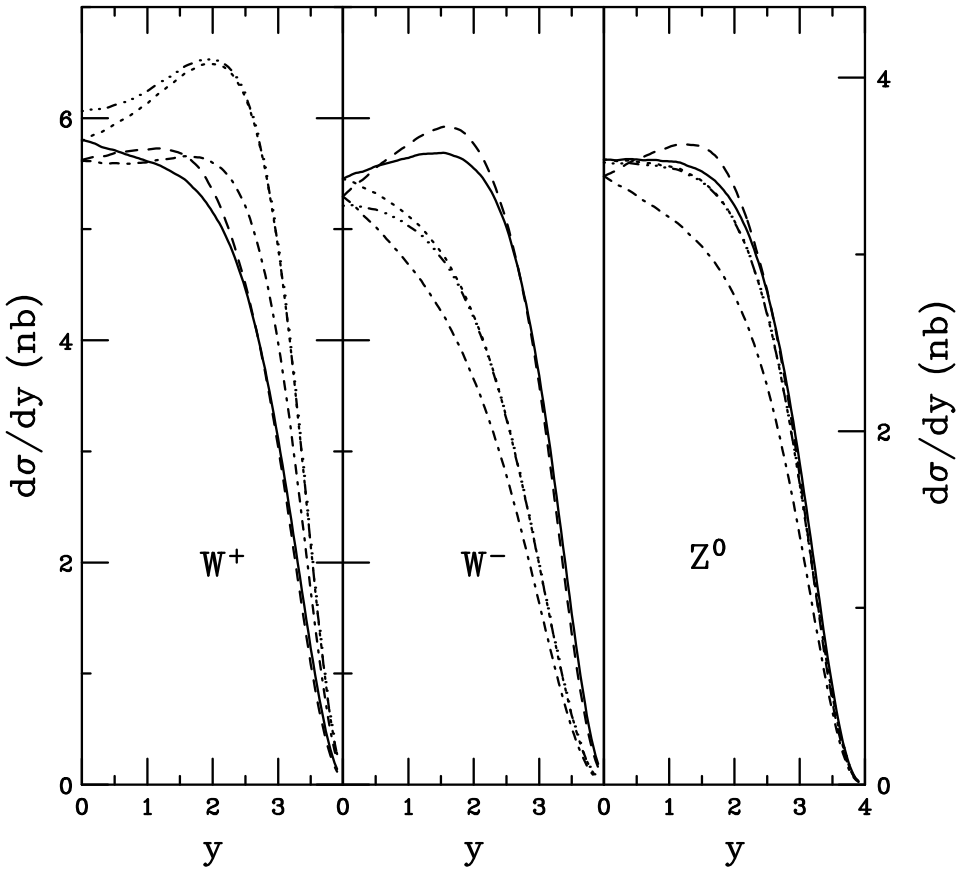

Figure 15: The W^+, W^- and Z^0 rapidity distributions in pp, pPb and Pbp collisions at 5.5 TeV/nucleon evaluated at $Q = M_V$. The solid and dashed curves show the results without and with EKS98 shadowing respectively in Pbp collisions while the dotted and dot-dashed curves give the results without and with EKS98 shadowing for pPb collisions. The dot-dot-dot-dashed curve is the pp result. [R.V., in pA working group part of Hard Probes Yellow Report.]

Photoproduction Comes For Free in Heavy Ion Collisions

- Strong electromagnetic fields surround accelerated nuclei
- Photon from field of one nucleus interacts with gluon from periphery of opposite nucleus
- Photons almost real, virtuality $q^2 < (\hbar c/R_A)^2$, small
- These photons can interact themselves (direct) or fluctuate into states with multiple $q\overline{q}$ pairs and gluons (resolved)
- Grazing collisions with rapidity gap could be clean signal for photoproduction measurements
- Heavy quarks, dijets and γ+jet probes alternative way to obtain nuclear parton distributions
- **Only thing needed to do this physics is to not throw away peripheral events**

Heavy Quark Photoproduction Probes Nuclear Gluon Distribution

$\gamma g \to Q\overline{Q}$ only direct process for photoproduction

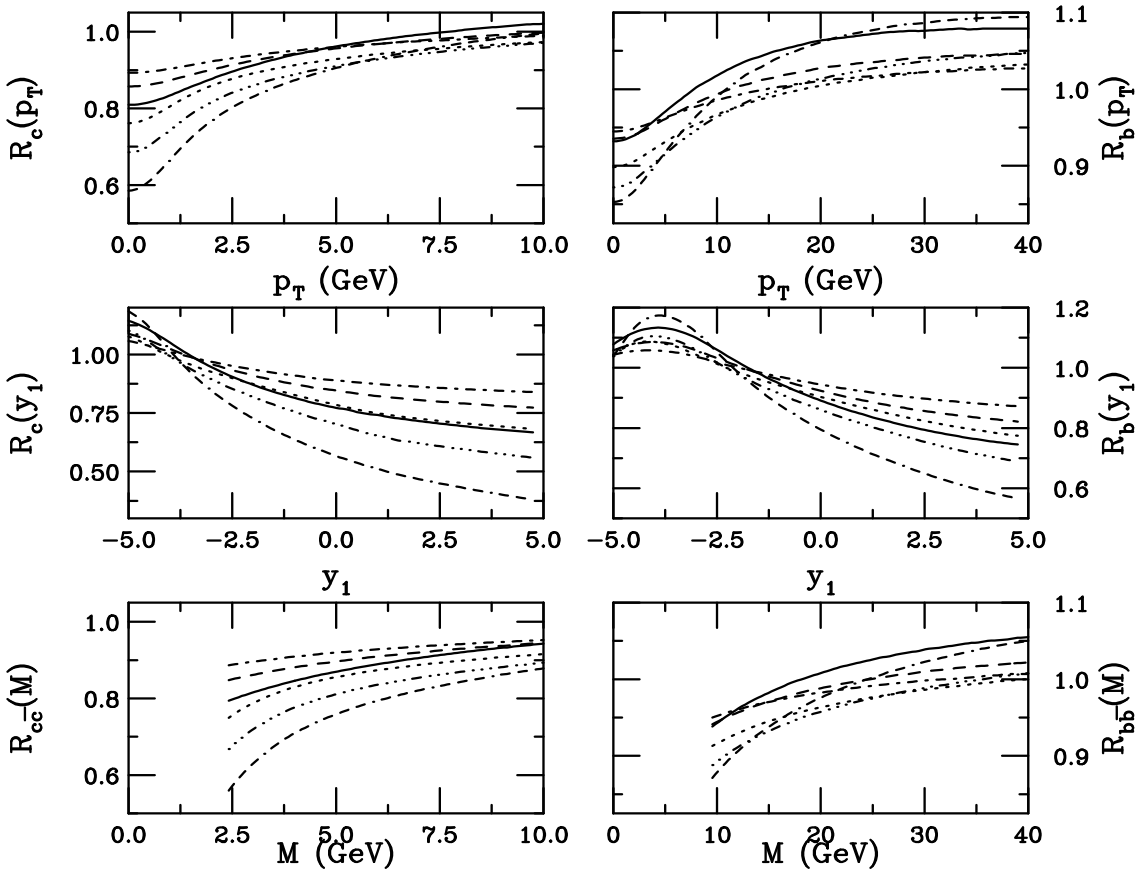

Figure 16: Shadowing in direct $Q\overline{Q}$ photoproduction in peripheral AA collisions. The left-hand side shows the results for charm while the right-hand side gives the results for bottom. The single Q p_T (upper) and rapidity (middle) ratios are shown along with the $Q\overline{Q}$ pair invariant mass ratios (lower). The results for the EKS98 (O+O (dot-dashed), Ar+Ar (dashed) and Pb+Pb (solid)) and FGS (O+O (dotted), Ar+Ar (dot-dot-dot-dashed) and Pb+Pb (dash-dash-dash-dotted)) shadowing parameterizations are given. The photon is coming from the left.

Resolved Component Small Relative to Direct

Even for most extreme case of gluon distribution in the photon (LAC1), resolved/direct ratio still below 1 over most of phase space

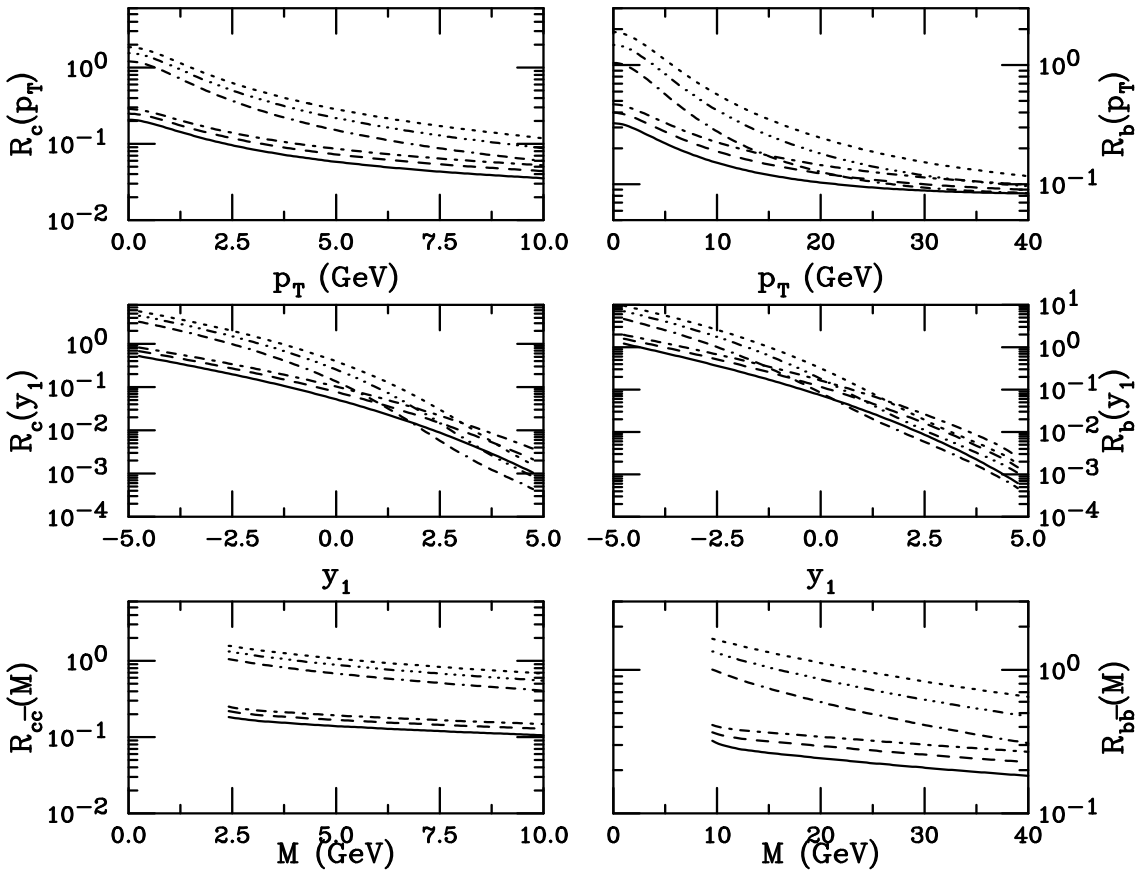

Figure 17: Resolved to direct $Q\overline{Q}$ photoproduction ratio in peripheral AA collisions. The left-hand side shows the results for charm while the right-hand side gives the results for bottom. The EKS98 shadowing parameterization is used in both cases. The single Q p_T (upper) and rapidity (middle) ratios are shown along with the $Q\overline{Q}$ pair invariant mass ratios (lower). The results for the GRV-G (O+O (dot-dashed), Ar+Ar (dashed) and Pb+Pb (solid)) and LAC1 (O+O (dotted), Ar+Ar (dot-dot-dot-dashed) and Pb+Pb (dash-dash-dash-dotted)) photon parton distributions are given. The photon is coming from the left.

Rates High

	$N_{Q\overline{Q}}$				
	GRV-G			LAC1	
AA	no shad	EKS98	FGS	no shad	EKS98
			$c\overline{c}$		
O+O	3.20×10^8	2.96×10^8	2.69×10^8	5.92×10^8	5.63×10^8
Ar+Ar	8.30×10^8	7.40×10^8	6.49×10^8	1.41×10^9	1.33×10^9
Pb+Pb	6.03×10^8	5.20×10^8	4.30×10^8	9.38×10^8	8.64×10^8
			$b\overline{b}$		
O+O	1.76×10^6	1.71×10^6	1.66×10^6	2.98×10^6	2.94×10^6
Ar+Ar	4.09×10^6	3.98×10^6	3.81×10^6	6.28×10^6	6.24×10^6
Pb+Pb	2.56×10^6	2.51×10^6	2.38×10^6	3.07×10^6	3.52×10^6

Table 7: Total $Q\overline{Q}$ photoproduction rates, integrated over $b > 2R_A$ in peripheral *AA* collisions. A 10^6 s run is assumed.

Summary

- Calculable initial state
- Hot, long lived QGP phase
- High rates for hard probes
- At the LHC we will study higher p_T processes than ever before
- Lead beams will turn into golden data